 ICCES, vol.4, no.1, pp.1-9, 2007

Experimental and Computational Investigation of Flow in a Periodically – Driven Cavity

S. Sriram[1], S. Pushpavanam[1], Abhijit P. Deshpande[1] and E.G. Tulapurkara[2]

Summary

The flow in a periodically-driven cavity is studied experimentally using Particle Image Velocimetry (PIV) and the results are compared with Computational Fluid Dynamics (CFD) simulations. The experiments are carried out in a cuboid of 0.1x 0.1m x 0.02 m size with glycerol as the fluid. Measurements are carried out at various amplitudes and frequencies of lid motion. The planar velocity measurements are made at three different z-planes and x-planes. It is found that the temporal variations of x-, y- and z-components of velocities of the flow are periodic, with the imposed plate frequency as the dominant frequency. Computation using FLUENT package show close agreement with experimental data. The effect of width of the cavity is studied using CFD simulations. Subsequently flow patterns in cases with different widths show similarities when a modified Reynolds number is used.

keywords: Particle Image Velocimetry, Cavity with periodically-driven lid, Secondary vortices

Introduction

The study of the fluid motion in a lid-driven cavity is a classical problem in fluid mechanics. It serves as a benchmark case for understanding complex flows with closed circulation. It also serves as an idealized representation of many industrial-process applications such as short-well and flexible blade coaters. In recent years, the flow in a cavity with oscillating lid is being examined as a bench mark case with higher level of complexity in flow and from the point of view of applications in mixing devices.

O'Brien [1] has carried out flow visualisation study in a box with oscillatory lid. However quantitative results are lacking. He has also carried out 2-D simulation which gives satisfactory comparison with flow visualisation results. The flow within a 2-D closed finite square cavity, driven by a sliding wall which executes sinusoidal oscillation was treated by Soh et al. [2]. Later Iwatsu et al. [3] studied square cavity driven by a torsionally oscillating lid through numerical simulations for a wide range of Reynolds number and frequency of the oscillating lid. They reported that at low frequencies the effect of the lid motion penetrates a larger depth into the cavity and flow is similar to the steady driven cavity flow at the maximum plate velocity. At high frequencies, however, the flow was confined within a thin

[1]Department of Chemical Engineering, Indian Institute of Technology Madras

[2]Department of Aerospace Engineering, Indian Institute of Technology Madras, Chennai - 600036, India; Corresponding author: **egt@ae.iitm.ac.in**

layer near the oscillating lid. Iwatsu et al. [4] analysed the 3-D flow structures in a cubic cavity with an oscillating lid by numerical simulations. They studied the effect of frequency on the penetration depth. They reported the presence of the secondary flows at low frequencies illustrating the 3-D nature of the flow.

In spite of various investigations described above, very few quantitative experimental studies have been carried out in periodically-driven cavities. Sriram et al. [5] investigated flow of Newtonian fluid in a periodically-driven cavity using Particle Image Velocimeter. They have reported temporal and spatial variations of the flow. Also presented is the evolution of secondary vortices at different plate position as a function of Reynolds number. In the present investigation measurements of all the three (u, v, w) components have been carried out at Re = 406. The results are compared with numerical simulation. Subsequently the effect of the width of cavity is studied numerically.

Experimental and Computational Details

The experiments are conducted in a periodically-driven cavity [5]. The walls are made of acrylic sheets of 0.6 cm thickness. The length (L) of the cavity along x direction is 0.1 m, the height (H) measured in y direction is also 0.1 m and the span wise width (W) of the cavity is 0.02 m in z direction (Fig. 1a).The front and side views of the cavity are shown in Fig. 1. The aspect ratio defined as the ratio of length to height (L/H) of the cavity is unity.

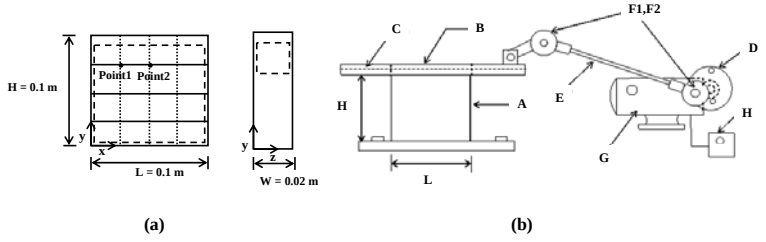

Figure 1: (a) Geometric details of the cavity, (b) Schematic diagram of the experimental setup.

Fig. 1(b) shows the front view of the cavity (A) and the experimental set up. The top plate (B) is designed to move to and fro along the x-direction motion .This was rendered possible with a guide plate (C) arrangement. The periodic motion is enabled a drive wheel (D) and connecting rod (E) assembly. Ball bearings (F1, F2) are used for attaching each end of the connecting rod as well as to support the drive wheel. A permanent magnet DC motor (G) is used to turn the drive wheel. The speed of the motor and hence frequency is controlled by a thyristor drive (H). The amplitude (maximum displacement) of the top plate motion is set by the radius at which the connecting rod is attached to the drive wheel. The velocity of the plate (U_p) is confirmed as sinusoidal using image analysis. i.e. $U_p = U_{max}\sin(\omega t)$,

where U_{max}= Aω, is the maximum plate velocity (m/s). Here 'A' represents the amplitude of the plate motion, 'ω' is the angular frequency which is given by 2πf where f is the measured frequency of the plate motion. The experiments are conducted at three different amplitudes viz. 0.045, 0.05 and 0.06 m and three different angular frequencies 0.9, 1.70, 2.51 s^{-1}. The Reynolds number is defined as Re = (U_{max} ρH)/μ and the Stokes number is defined as St = $\omega\rho H^2/\mu$. The maximum velocity of the plate (U_{max}= Aω) is the velocity scale, H is the depth of the cavity (Fig. 1), ρ is the fluid density and μ is the viscosity of the fluid. The experimental fluid is a mixture of commercial 99% glycerol and water. The viscosities were measured at 25 ^{0}C, using a Rheometer Physica MCR-301 and the corresponding viscosities are found to be 0.0116 Pa.s (50 vol %), 0.0143 Pa.s (60 vol %). The volume % reported here is for glycerol.

Experimental Technique

Particle Image Velocimetry (PIV), a non-intrusive technique, is used to get accurate quantitative information of the instantaneous planar velocity field. The setup is supplied by M/s. LaVision GmBH, Germany. The fluid is seeded with hollow glass particles of 5 - 10 μm size. The PIV measurements are made using 1mm thick Nd: YAG laser sheet, of 120 mJ pulse energy and 532 nm wavelength, to illuminate the plane of interest. The light scattered by the particles is recorded with FlowMaster-3S charge coupled device (CCD) camera (1280 x 1024 pixels, 8 Hz). The PIV acquisition rate is 4 Hz. The 2-D velocity field measurements in the x-y plane (u - velocity in x direction, v - velocity in y direction) and y-z plane (w-velocity in z direction) are carried out in fields of view of 0.096 m $\times$0.092 m and 0.022 m$\times$0.018 m respectively. Two images are taken within a short interval of time. Each image is subdivided into interrogation windows of size 32$\times$32 pixels. The size of each interrogation window is 3.0 mm$\times$2.8 mm. The cross correlation function for each interrogation window is used to obtain a two-dimensional shift. Subsequent division by time interval between the two consecutive images yields the velocity components in the imaging plane. The time interval between two laser pulses for various experiments varied between 0.014 - 0.12 s.

The motion of the top plate is measured experimentally. Since this motion is periodic the velocities at different points in the flow field also show similar variations. This data is used for a quantitative comparison between the results of experiments and numerical simulations. We describe the flow field at four different positions of top plate. At position 1, the plate moves from the extreme right towards the center. Position 2 corresponds to the plate at the center of the cavity moving towards the left and position 4 corresponds to the plate at the center of the cavity moving towards the right. At both positions 2 and 4, the plate velocity is at its maximum, though in the opposite directions. The plate position when it moves from the left

extreme towards the center is called position 3. The experimental data are collected after the initial transients have decayed, typically after five minutes.

Computational Technique

The CFD simulations are performed using Fluent 6.1 software. The 3-D quad-map grid is obtained using Gambit 2.1. The grid independent results are obtained with 200,000 ($100\times100\times20$) cells. A periodic boundary condition on the top plate is imposed using an externally defined macro. The other faces of the cavity are considered as solid stationary walls. In the code the convective terms are discretized using second order up winding and the coupled implicit time formulation has second order accuracy.

Results and Discussion

The planar measurements are made over a broad range of parameters. The area of experimental investigation is shown as dashed lines in Fig. 1. The measurements in x-y plane are carried out at different z planes viz. z = 0.005, 0.01 and 0.015 m i.e. at a quarter, half and three quarters of the width of cavity. Similarly the measurements were done at different x planes x = 0.025, 0.05 and 0.075. The magnitudes of u and v at different points are extracted from the instantaneous velocity fields measured in x-y plane and magnitude of w from the velocity fields measured in y-z plane. All the results discussed in this work are obtained after the decay of initial transients. The instantaneous planar velocity fields at each plate position are averaged over ten cycles and used for the analysis. The non-dimensional velocities are defined as, $u^* = u/U_{max}$, $v^* = v/U_{max}$and $w^* = w/U_{max}$ respectively. Time is non-dimensionalised with the frequency of the plate motion, $t^* = t\times\omega$. The results of experiments and simulations for Re = 406 are presented in the next section.

Re = 406

Figures 2a and b present the variations of, u* and v* at points 1 and 2 (see Fig. 1 for location of points) as obtained form PIV measurements and CFD simulations. The magnitude of z- component velocity (w*) is found to be very small and is not presented. Point 1 is closer to the top corner and both u* and v* have significant amplitudes. Point 2 lies in the central plane and v* is smaller than u*.The computed results agree closely with experimental results. The computed amplitudes at point 1 are slightly higher than the experimental results. At point 2 the mean value of v* is smaller in computations.

In order to get some insight into the existence of dominant frequencies, the power spectrum analysis is carried out. Figure 3 shows the comparison of power spectra of u* and v* at points 1 and 2 obtained from experiments. In case of u*, a dominant frequency of $f_1 = 0.15\ s^{-1}$, close to imposed plate frequency is observed at both the points 1 and 2. In case of v*, a dominant frequency of $f_1 = 0.15\ s^{-1}$ is observed at point 1. However at Point 2 a peak is observed at $f_2 = 0.3\ s^{-1}$, which is

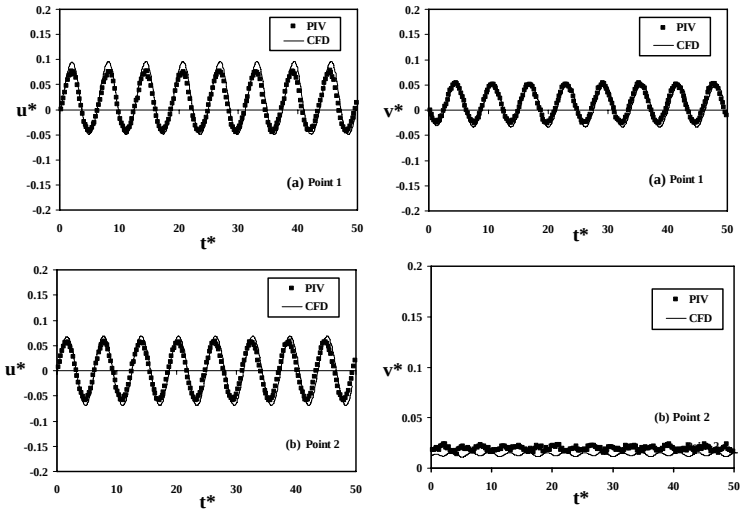

Figure 2: Comparison of temporal variation of u* and v* from PIV measurements and CFD simulations, Re =406, St=895: (a) Point 1 (b) Point 2.

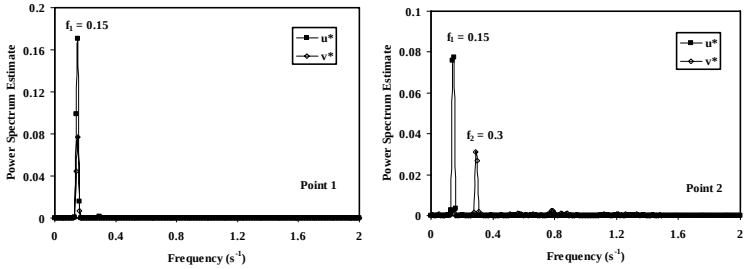

Figure 3: Power spectra of u* and v* from experiments at points 1 and 2, ω = 0.9 s^{-1}, Re =406, St = 895.

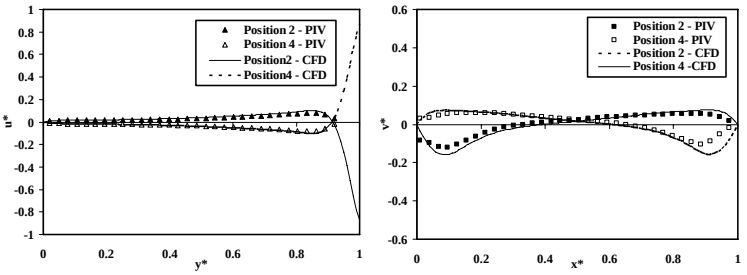

Figure 4: Comparison of computed and experimental results, Re = 406, St = 895, A = 0.045 m, ω = 0.9 s^{-1}: (a) * along a vertical line at x = 0.05 and z = 0.01 (b) v* along a horizontal line at y = 0.075 and z =0.01.

twice the imposed plate frequency.

The profiles of u* from the PIV measurements along a vertical plane at x = 0.05 and along the line at z =0.01 are shown in Fig. 4(a). The profiles shown are for the plate position 2 and 4, i.e. when the magnitude of plate velocity is maximum. The vertical coordinate is non-dimensionalised by the scale, y* = y/H. It is seen that u*is maximum near the plate as expected and gradually decays along the depth of the cavity. It is interesting to note that the velocity profiles at positions 2 and 4 are opposite to each other. This is due to the symmetry of the domain and the sinusoidal variation of the plate velocity. There exists a counter flow and large fraction of fluid moves in a direction opposite to the plate motion (Fig. 5). The velocity profile of v* along a horizontal line at y = 0.075 and z = 0.01 at plate positions 2 and 4 are also shown in Fig. 5(b). The horizontal coordinate is non-dimensionalised using the length of the cavity (L) as the reference scale i.e. x*= x/L. Profiles of v* at positions 2 and 4 are nearly mirror images, about x = 0.05. The profiles from CFD simulations are in close agreement with the experimental results.

The streamline patterns from PIV measurements and CFD simulations are shown in Fig. 5. Recirculation regions, near the top corner of the cavity are observed at positions 1 and 3. However at positions 2 and 4 (i.e. at maximum plate velocity) there exists only a primary vortex which fills up the entire cavity. The streamline patterns for Re=1250 are shown in Fig. 6. Secondary vortices appear even in positions 2 and 4.

Effect of cavity width

Having validated the code, the influence of the width of the cavities in z direction is examined by computations. The CFD simulations are performed for cavities of width, W = 0.01 m and W = 0.03 m (recall span width of experimental cavity is 0.02m). Figure 7(i) (a, b) show the streamline patterns at different plate positions for Re = 1250. For W =0.01 the secondary vortex is not seen for positions 2 and 4. However for W =0.03, the secondary vortices are larger in size than when W is 0.02. This suggests the impact of the width of the cavity on the overall flow. This can be due to the fact that span width is not accounted for in the length scale of the defined Reynolds number. Following Leong and Ottino [6], Reynolds number was redefined as $Re^* = (U_{max}\rho W/\mu) \times (W/H)^{1/2}$. The simulations were done for different span width by keeping U_{max}constant.

The computations are repeated for W =0.01m and W =0.03 m, keeping Re* same. While doing so since W/H changes in both the cases, μ was varied to keep Re* constant. When μ is chosen equal to 0.143 Pa.s and W =0.02, Re is 1250 and the corresponding Re* is 106. To keep the same Re* for W = 0.01 and W =0.03 m, the values of μ were changed to 0.0058 and 0.0264 Pa.s respectively. This gives Re of 2900 for W =0.01m and Re = 665 for W =0.03 m. The streamline patterns

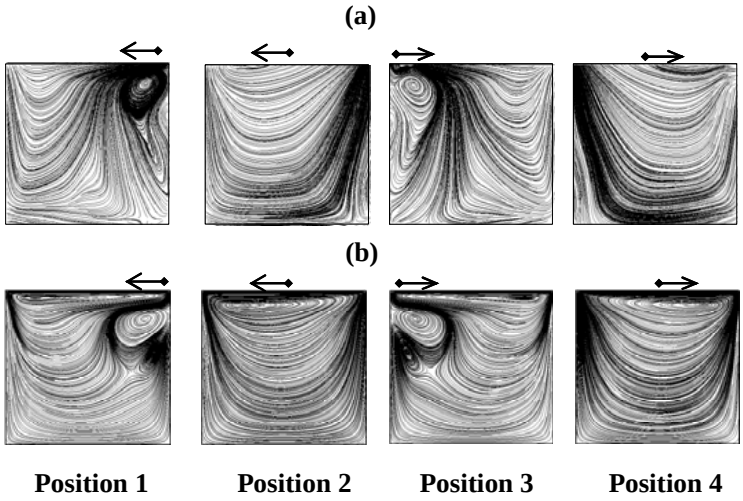

Figure 5: Streamline patterns at four positions of top plate, Re = 406, A = 0.045 m, $\omega = 0.9\ s^{-1}$: (a) PIV measurements and (b) CFD simulations

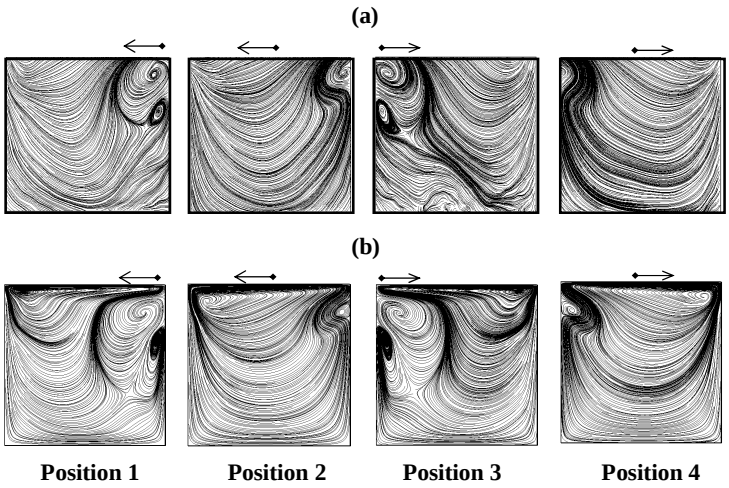

Figure 6: Streamline patterns at four positions of top plate, Re = 1250, A = 0.06 m, $\omega = 2.5\ s^{-1}$: (a) PIV measurements and (b) CFD simulations

are shown in figures 7(ii) (a, b). It is interesting to note that the streamline patterns in Figs. 6 (b), 7(ii) (a, b) are nearly the same which shows appropriateness of Re* as the non-dimensionalisation parameter of the flow.

Conclusions

The periodic flow in a three dimensional cavity with oscillating lid has been studied under different experimental conditions using Particle Image Velocimetry.

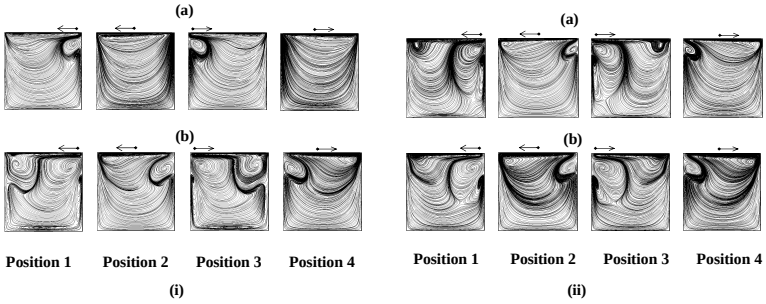

Figure 7: Computed streamline patterns for different cavity widths for (a) W = 0.01m (b) W = 0.03 m: (i) Re = 1250 and (ii) Re*= 106

The temporal variations of the flow at characteristic points display the sinusoidal variation. The experimental results are compared with 3-D computational fluid dynamic simulations and good agreement is observed. The effect of span width on the flow behaviour is studied by performing simulations with cavities of different widths. It is observed that span width should be included in the length scale while defining non-dimensional parameters.

Acknowledgement

The measurements were carried out using DST (Department of Science and Technology) supported flow visualisation facility. The fourth author thanks AICTE (All India Council for Technical Education) for fellowship which enables him to work at IIT Madras.

References

1. O'Brien V., 1975, "Unsteady cavity Flows: Oscillatory Flat Box Flows[1]" Journal of Applied Mechanics, Transactions of ASME, 557-563.

2. Soh, W. H., and Goodrich, J. W., 1988, "Unsteady Solution of Incompressible Navier-Stokes Equations," Journal of Computational Physics, **79**, 113-134.

3. Iwatsu, R., Hyun, J.M. and Kuwahara, K., 1992, "Numerical Simulations of flows driven by a Torsionally Oscillating Lid in a Square Cavity," Journal of Fluids Engineering, **114**, 143-151.

4. Iwatsu, R., Hyun, J.M. and Kuwahara, K., 1993, "Numerical Simulations of Three Dimensional Flows in a Cubic Cavity with an Oscillating Lid," Journal of Fluids Engineering, **115**, 680-686.

5. Sriram, S., Deshpande A. P., and Pushpavanam S., 2006, "Analysis of spatio-temporal variations and flow structures in a periodically-driven flow," Journal of Fluids Engineering, **128**, 413- 420.

6. Leong C. W., Ottino J. M., 1989, "Experiments on mixing due to chaotic advection in a cavity," Journal of Fluid Mechanics, **209**, 463-499.